Multiplet Structure Investigation of the L-Series Lines of Rare Earth Elements

V. F. DEMEKHIN, A. I. PLATKOV, AND M. V. LYUBIVAYA

Rostov State University

Submitted June 28, 1971

Zh. Eksp. Teor. Fiz. **62**, 49–56 (January, 1972)

A longwave X-ray spectrograph was used to investigate the L-series lines of rare earth elements in R_2O_3 oxides. Considerable asymmetry and multiplicity of the $L_{\alpha_{1,2}}$, L_{β_1}, $L_{\beta_1'}$, and L_{γ_1} lines is observed. A calculation of the multiplet structure of the $d^9 4f^n$ configuration is performed for $58 \leq Z \leq 71$ in the intermediate coupling approximation. Transition probabilities of 3d and 4d electrons from multiplet levels to the 2p state are calculated. The shapes of the $I_{\alpha_{1,2}}$, L_{β_1}, L_{B_2} and L_{γ_1} x-ray lines of the rare-earth elements in R_2O_3 oxides are explained.

THE present paper is devoted to an experimental and theoretical investigation of the shapes of the rare-earth element L-series lines. It was shown in[1] that the complicated shape of the L_{β_2} and L_{β_1} lines of Dy in Dy_2O_3 can be attributed to the splitting of the states of an atom with vacancy in the 4d shell as a result of exchange interaction of the 4d electrons with the electrons of the unfilled 4f shell. Since there are no investigations of the shape, width and asymmetry of the rare-earth element L-series lines, it seemed desirable to perform this study.

EXPERIMENTAL RESULTS

By using a DRS (long-wave x-ray) spectrograph with a quartz ($[10\bar{1}0]$) analyzer, we obtained the $L_{\alpha_{1,2}}$, L_{β_1}, L_{β_2}, and L_{γ_1} lines of all the rare-earth elements (with the exception of $_{61}$Pm) in oxides of the R_2O_3 type. The spectra were excited with a 10-mA beam of 20-kV electrons. The spectra were recorded photographically. The resolution was 14 000. There were no traces of melting in the focal spot of the aluminum fitting of the anode, and it can therefore be assumed that the sample temperature during the exposure time was much lower than the oxide-decomposition temperature[2]. All the rare-earth-element spectra were corrected after photometry for the densitometric characteristic constructed in accordance with the method of[3]. The results obtained after averaging several spectra are shown in Figs. 1 and 2 and in the table.

An examination of the figures and of the table shows that the shape of the investigated lines changes significantly on going from one element to another. Let us examine the main features of the spectra. Starting with $_{59}$Pr, there appears on the long-wave side of the L_{β_2} line a weak line having an energy that coincides with the energy of the non-diagram line $L_{\beta_{14}}$[4]. With increasing z, the distance between the L_{β_2} and $L_{\beta_{14}}$ lines increases up to $_{65}$Tb, when the $L_{\beta_{14}}$ is separated from the L_{β_2} line. With further increase of Z, the distance decreases and, starting with $_{67}$Ho, the L_{β_2} and $L_{\beta_{14}}$ lines are practically inseparable. The width of the L_{β_2} line, measured at half the intensity of the maximum, increases from $_{58}$Ce to $_{60}$Nd, then stays in the range from 7 to 8 eV, after which it increases from $_{66}$Dy to $_{69}$Tu, reaching a value 17 eV. The width then decreases sharply and its value for the last element of the rare-earth group, $_{71}$Lu, is 10.2 eV, which practically coincides with the widths of the L_{β_2} lines of the elements with $71 < Z \leq 77$ (9.9–9.7 eV)[5].

The intensity of the $L_{\beta_{14}}$ line increases weakly with increasing Z, amounting to 0.2–0.4 of the intensity of the L_{β_2} line; starting with $_{67}$Ho, this quantity cannot be determined. The L_{β_2} line of all the elements of the rare-earth group is asymmetrical, and the asymmetry index is always larger than unity. The largest asymmetry is possessed by the lines of the end of the group, although the L_{β_2} line of $_{71}$Lu becomes symmetrical.

On the long-wave side of the L_{γ_1} line, starting with $_{59}$Pr, there is observed a distinct line that coincides in energy with the energy of the non-diagram L_{γ_9} line[4]. The distance between this line and L_{γ_1} varies by several eV in the series of rare-earth elements, amounting to about 20 eV. Starting with $_{68}$Er, the L_{γ_1} and L_{γ_9} lines merge to form a broad line of complex shape. The width of the L_{γ_1} line increases monotonically with increasing Z, and is larger than the width of the L_{β_2} lines for all the rare-earth elements. The intensity of L_{γ_9} increases with increasing Z and its value for Tb and Dy is on the order of 0.7–0.8 of the intensity of L_{γ_1}. It should be noted that the intensity ratio $IL_{\gamma_9}/IL_{\gamma_1}$ is larger than the ratio $IL_{\beta_{14}}/IL_{\beta_2}$ for all the elements. The elements whose L_{γ_9} is well separated from L_{γ_1} reveal an asymmetry and a structure in the L_{γ_1} lines, and the asymmetry index is smaller than unity.

An investigation of the shape of the L_{β_1} lines has shown that almost all of them have a weakly pronounced multiplet structure and a protracted long-wave branch. The asymmetry index of all the L_{β_1} lines is larger than unity, and the width for the elements of the second half of the group is larger than for the elements that follow the rare-earth group. The non-diagram line $L_{\beta_1'}$ is observed for most elements on the short-wave side of the L_{β_1} line. It should be noted that the distance between the lines L_{β_1} and $L_{\beta_1'}$ is smaller by several eV than the dis-

Z	$\Delta E(\alpha_1-\alpha_2)$, eV	$\Delta E(\beta_1-\beta_2')$, eV	Γ_{α_1}, eV	Γ_{α_2}, eV	Γ_{β_1}, eV	a_{α_1}	a_{β_1}	$\Delta E(\beta_2-\beta_{15})$, eV	Γ_{β_2}, eV	a_{β_2}	$\Delta E(\gamma_1-\gamma_5)$, eV	Γ_{γ_1}, eV	a_{γ_1}
$_{58}$Ce	18.7		5.6	5.2	5.7	1.6	1.3		5.9	1.1		5.8	1.0
$_{59}$Pr	20.4		5.5	6.2	6.6	1.0	1.3		7.0	1.0		7.5	1.0
$_{60}$Nd	22.1	16	5.5	5.5	7.8	1.7	1.8		6.9	1.3	19	7.2	0.8
$_{62}$Sm	27.3	21	6.6	6.0	7.6	1.1	1.5		6.4	1.5	23	8.8	0.8
$_{63}$Eu	28.4	21	7.0	6.5	8.8	1.3	1.4	25	7.8	1.9	21	10.2	0.7
$_{64}$Gd	30.0	22	7.3	7.5	7.0	1.5	1.3	25	7.2	1.5	21	10.9	0.5
$_{65}$Tb	34.9	28	7.9	7.7	7.5	1.3	1.1	26	8.3	1.3	22	11.0	1.0
$_{66}$Dy	36.8	28	9.2	8.2	8.3	1.5	1.6	24	8.9	1.5	18	16.4	
$_{67}$Ho	40.7	35	9.7	7.3	7.8	1.7	1.5		9.4	1.6	19	20.1	
$_{68}$Er	43.2		10.0	8.8	7.3	1.7	1.4		11.5	2.2		27.4	
$_{69}$Tm	46	38	10.1	7.7	8.1	1.5	1.1		17.0	2.8		22.1	
$_{70}$Yb	48		9.1	7.2	7.7	1.2	1.0		14.6	1.9		17.3	
$_{71}$Lu	51		6.2	5.8	7.2	1.1	1.2		10.2	1.0			

Γ–line width, a–asymmetry coefficient.

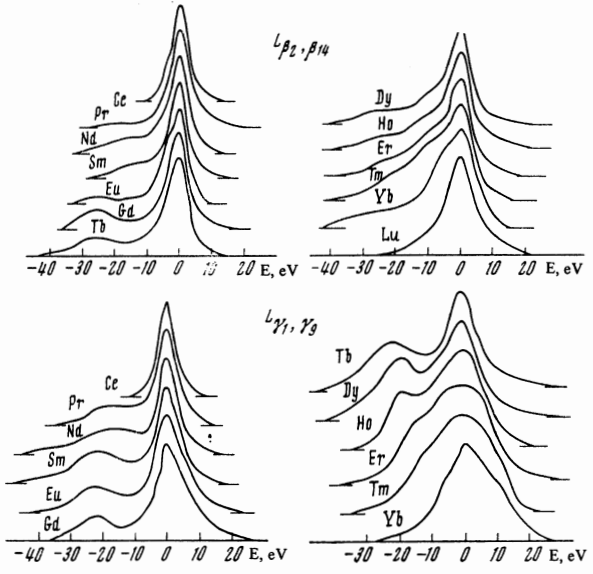

FIG. 1. Spectra of $L_{\beta_2,\beta_{14}}$ and L_{γ_1,γ_9} lines.

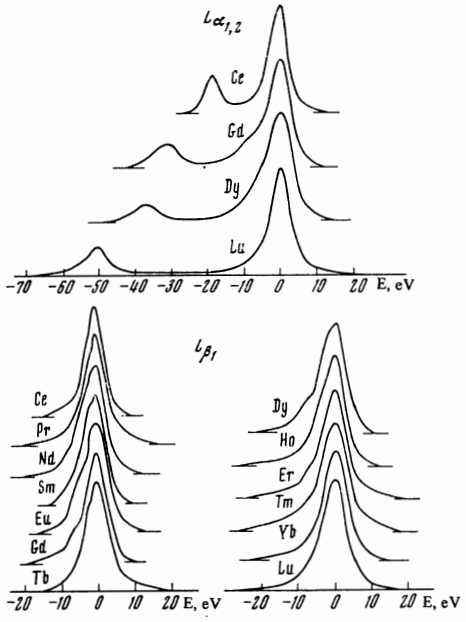

FIG. 2. Spectra of L_{β_1} and $L_{\alpha_{1,2}}$ lines.

tance between the $L_{\alpha_{1,2}}$ lines.

An investigation of the shape of the $L_{\alpha_{1,2}}$ doublet has shown that both L_{α_1} and L_{α_2} are asymmetrical; the asymmetry index is always larger than unity. The widths of the L_{α_1} lines increase with increasing Z from 5.5 to 10 eV, and decrease strongly at the end of the group. The widths of the L_{α_1} lines are larger than the widths of the L_{β_1} and L_{β_2} lines, and are larger for all elements of the second half of the group than for the elements with $Z > 71$. The ratio of the intensities of the L_{α_1} and L_{α_2} lines is ~5. Figure 2 shows typical $L_{\alpha_{1,2}}$ lines.

CALCULATION SCHEME AND RESULTS

Figure 3 shows a comparison of the line widths of the L series and of the magnetic moments of triply-charged ions as functions of the atomic number[6]. We see that larger line widths are possessed by elements with larger magnetic moments. This suggests that the interaction of the 4f electrons with the unfilled internal shell exerts an appreciable influence on the structure of the x-ray levels. We have performed a simplified calculation of the multiplet structure of the states mentioned above. The simplification consisted of expressing the exchange part in the Coulomb interaction of the d and f electrons in terms of the average exchange interaction, the energy of which was calculated after Condon and Shortley[7]; its value turned out to be $\overline{G} = 3G_1 + 12G_3 + 66G_5$. The electrostatic part of the Coulomb interaction for any pair of d and f electrons was assumed equal to the average energy of the electrostatic interaction[1)].

Inasmuch as the electrostatic part of the Coulomb interaction does not cause splitting in this case, such an approximation makes it possible to simplify greatly the problem of calculating the multiplicity of the x-ray levels, although one cannot claim the results to be complete or highly accurate, since the approximation is valid only for the case of seven unpaired 4f electrons. The states of the configuration $d^9 4f^n$, where n is the number of unpaired 4f electrons, have been characterized in the calculation by the quantum numbers m_l and m_s of the missing d electron, by the total spin S′ of the 4f shell, and by its projection. The orbital number of

[1)]A similar approximation was made by Nefedov[8] in the calculation of the multiplicity of the K spectra of the elements with $21 \leq Z \leq 30$.

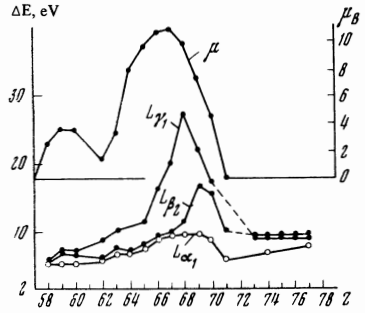

FIG. 3. Comparison of the dependences of the magnetic moments of triply-charged ions [3] and of the widths of the L-series lines on the atomic number.

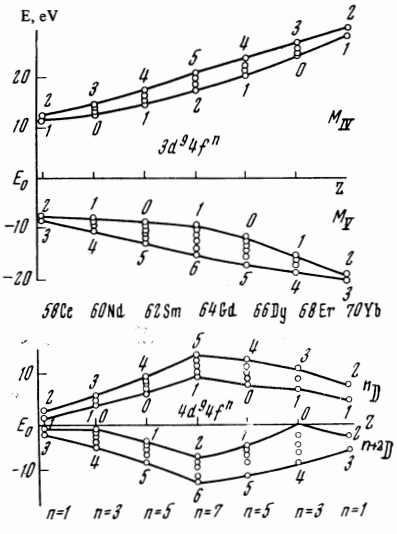

FIG. 4. Multiplet structure of the energy levels of the configurations $3d^9 4f^n$ and $4d^9 4f^n$ for rare-earth elements. The points show the positions of the levels that have values of J between the maximum and the minimum.

the 4f shell was not used for the description of the states. This basis was used to write down the wave functions of the states characterized by the numbers L, S, J, and M_j (the LS-coupling scheme). Here L = 2, S = (n ± 1)/2 is the total spin, and J is the resultant angular momentum of the configuration.

The parameters ζ_d of the spin-orbit interaction used for the numerical calculation of the energies of the multiplets of the $3d^9 4f^n$ and $4d^9 4f^n$ configurations were taken from the work of Herman and Skillman[9], while the numerical values of the integrals G_k were obtained by interpolating their values for Nd, Sm, and Dy; the latter were calculated with the aid of wave functions from[9]. The results of the calculation are shown in Fig. 4.

After analyzing the obtained formulas, we found a general expression for the energy of the sublevels of the multiplets for any number of unpaired 4f electrons

$$E(^{2S+1}L_J) = E_0 + {}^1/_2\overline{G} + {}^1/_4\zeta_d \pm {}^1/_2[(n+1)^2\overline{G}^2 + a\overline{G}\zeta_d + j_m{}^2\zeta_d{}^2]^{1/2}.$$

Here

$$a = 2J(J+1) - {}^1/_2 n(n+2) - 2j_m{}^2,$$

n is the number of unpaired 4f electrons, $j_m = 5/2$ is the largest j for the d electron, J is the total angular momentum of the configuration, S is the total spin of the configuration, and E_0 is the average energy of the configuration. The square root is taken with a positive sign for the levels of ^nD terms and with negative sign for ^{n+2}D. With a suitably modified notation, the formula also describes the energies of the $p^5 4f^n$ configuration.

An examination of Fig. 4 shows that the $3d^9 4f^n$ configuration has two multiplets which are genealogically connected with the M_V and M_{IV} levels, since the distances between them are determined mainly by the spin-orbit interaction of the 3d electron. The energy splitting of these multiplets increases towards the middle of the group of the rare-earth elements and then decreases, amounting to 6 eV for the M_V multiplets and up to 3 eV for the M_{IV} multiplets.

Since the wave functions describing the states genealogically related to the M_V level (there is no 3d electron with j = 5/2) contain an admixture of wave functions of states with vacancies j = 3/2, while the functions describing states originating from the M_{IV} level have an admixture of functions with vacancy j = 5/2, the customarily employed x-ray designations are not correct in this case. We retain them, however, for convenience.

For the $4d^9 4f^n$ configuration, the exchange interaction leads to the appearance of two terms, ^nDn and ^{n+2}D. The distance between them increases sharply with increasing Z, up to $_{64}Gd$ (~20 eV), and then decreases slowly. It is clear that the increase of the distance between terms is due to the increase in the number of unpaired 4f electrons and in the average exchange-interaction energy with increasing Z. A further increase of the exchange energy is cancelled out by a decrease in the number of unpaired 4f electrons. The x-ray designations N_{IV} and N_V are not suitable for a description of the states of this configuration.

COMPARISON WITH EXPERIMENT

It is clear from the calculation of the energy multiplets that when the d electron goes over into the 2p state, doublets with a complex fine structure should be emitted. A comparison of the calculated and experimentally obtained interdoublet states has made it possible to relate the lines L_{γ_1} and L_{γ_9} with the transitions of the 4d electron from the terms ^{n+2}D and ^nD to the L_{II} level, and the lines L_{β_2} and $L_{\beta_{14}}$ with transitions from the same terms to the L_{III} level.

To explain the shapes of the L-series lines, we calculated the probabilities of transitions between the multiplets of the $4d^9 4f^n$ and $3d^9 4f^n$ configurations on the one hand and $2p^5 4f^n$ on the other. To this end, we constructed additionally the wave functions of the multiplets of the $2p^5 4f^n$ configuration in an approximation in which only the spin-orbit interaction of the 2p electron was taken into account. In the limiting cases of the LS and jj couplings (respective configurations $4d^9 4f^n$ and $3d^9 4f^n$), the probabilities, and consequently also the line intensities in the multiplets, turned out to be proportional to the statistical weights of the corresponding levels of the aforementioned configurations. The ratio of the probabilities of transitions from the terms ^nD and ^{n+2}D turned out to be n/(n + 2) for both the L_{β_2} and L_{β_1} lines, and $IL_{\alpha_1} : IL_{\alpha_2} : IL_{\beta_1} = 9 : 1 : 5$.

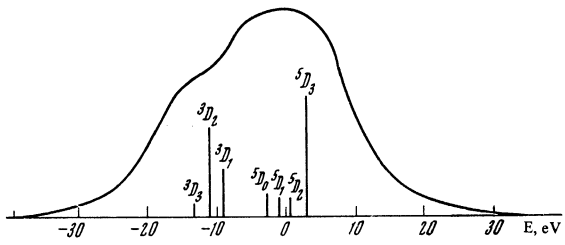

FIG. 5. Comparison of the experimental contour of the $L_{\gamma_{1,9}}$ band of $_{68}Er$ in Er_2O_3 with the calculation. The heights of the vertical lines are proportional to the transition probabilities. The letters denote the levels of the $4d^9 4f^n$ configurations the transitions from which cause the radiation.

However, on going over to the intermediate coupling, significant changes occur in the probability ratios. The general tendencies of these changes are as follows. The probability of the transitions from the term ^nD to the L_{II} level increases (L_{γ_9} line) and decreases for transitions to the L_{III} level ($L_{\beta_{14}}$ line). It follows therefore that the long-wave part of the L_{γ_1} line (L_{γ_9}) should be much more intense than the long-wave part of the L_{β_2} line ($L_{\beta_{14}}$). This agrees with the experimental fact that $IL_{\gamma_9}/IL_{\gamma_1} > IL_{\beta_{14}}/IL_{\beta_2}$. A calculation of the relative intensities of the lines in the multiplet shows that the L_{β_2} line should be much more asymmetrical than L_{γ_1}. Whereas the asymmetry coefficient of the L_{β_2} line is always larger than unity, L_{γ_1} can also have values smaller than unity. In the experiment, L_{β_2} is always asymmetrical on the long-wave side, and L_{γ_1} on the short-wave side.

From the calculations of the probabilities and of the structure it follows that the distance between the most intense components of the multiplets ^nD and ^{n+2}D in transitions to the L_{II} level is always smaller than in transitions to L_{III} level. This explains why the experimentally observed distance between L_{γ_1} and L_{γ_9} is smaller than the distance between L_{β_2} and $L_{\beta_{14}}$. Figure 5 shows a comparison of the experimental contour of the L_{γ_1,γ_9} band of $_{68}Er$ with the calculated positions and intensities of the multiplet components emitted by transitions between the configurations $2p^5_{1/2}4f^n$ and $4d^94f^n$. An examination of the figure shows good agreement between calculation and experiment.

On going over to the intermediate coupling, the probability ratio of the transitions from the M_V and M_{IV} multiplets to the L_{III} level decreases significantly. This explains why $IL_{\alpha_1}/IL_{\alpha_2}$ has a value on the order of 5 instead of 9. Simultaneously, there appears an appreciable probability of the transition from the M_V multiplet to the L_{II} level. This is connected with the fact that the wave functions of the M_V multiplet are linear combinations of the functions of the $3d^9_{5/2}4f^n$ and $3d^9_{3/2}4f^n$ configurations. As a consequence, a weak line $L_{\beta_1'}$, corresponding to a transition from the M_V multiplet to the L_{II} level should appear on the short-wave side of the L_{β_1} line. The distance between $L_{\beta_1'}$ and L_{β_1} should be smaller by several eV than the distance between L_{α_1} and L_{α_2}, since the peaks of the $L_{\alpha_{1,2}}$ lines are determined by the positions of certain levels in the multiplets, and the positions of the peaks of L_{β_1} and of the aforementioned line by the positions of others, the distance between the latter being smaller.

It follows from the table that the width of the L_{α_1} line is larger than the width of the L_{β_1} and L_{α_2} lines. This is connected with the fact that the M_V multiplet, which characterizes the final state in the emission of the L_{α_1} line, has a larger number of components and is more strongly split than M_{IV}.

It follows from the calculation that the asymmetry coefficient of the L_{α_1} line should be larger than unity, while the L_{β_1} line can have either long-wave or short-wave asymmetry. Experiment confirms this conclusion concerning the asymmetry of the L_{α_1} line, and for the L_{β_1} line the asymmetry coefficient is smaller than unity for all elements. Thus, although the approximations made in the calculation did not make it possible to obtain complete quantitative agreement with experiment, the results of the calculations explain the main regularities in the spectra and make it possible to interpret the $L_{\beta_{14}}$, L_{γ_9}, and $L_{\beta_1'}$ lines, which were previously regarded as non-diagram lines. Better agreement between calculation and experiment is observed for elements with a large number of 4f electrons. This is apparently connected with the fact that for a large number of 4f electrons, replacement of the energies of the true Coulomb interaction of the hole in the d shell with the 4f electrons by the average energy does not lead to large errors.

In conclusion we consider it our pleasant duty to thank V. V. Krivitskiĭ for kindly calculating the values of the integrals G_k.

[1]V. F. Demekhin, Izv. Akad. Nauk. SSSR, Ser. Fiz. (in press).

[2]V. V. Serebryakov, Khimiya redkozemel'nykh élementov (Chemistry of the Rare-Earth Elements), Vol. 1, Tomsk, 1959.

[3]V. F. Demekhin and I. Ya. Kudryavtsev, Rentgenovskie spektry i e'lektronnaya struktura veshchestva (X-Ray Spectra and the Electronic Structure of Matter), Vol. 2, Kiev, 1969, p. 100.

[4]É. E. Vaĭnshteĭn and M. M. Kakhana, Spravochnye tablitsy po rentgenovskoĭ spektroskopii (Reference Tables for X-Ray Spectroscopy), 1953.

[5]M. A. Blokhin, Fizika rentgenovskikh lucheĭ (The Physics of X-Rays), Gostekhizdat, 1957.

[6]S. V. Vonsovskiĭ and Yu. A. Izyumov, Usp. Fiz. Nauk **77**, 377 (1962) [Sov. Phys. Usp. **5**, 547 (1963)].

[7]U. Condon and G. H. Shortley, The Theory of Atomic Spectra, Cambridge, U. P., 1944.

[8]V. I. Nefedov, Izv. Akad. Nauk SSSR Ser. Fiz. **28**, 861 (1964).

[9]F. Herman and S. Skillman, Atomic Structure Calculations, New Jersey, 1963.

Translated by J. G. Adashko
8